



# Preparation and Characterization Studies of Dorzolamide-Loaded Ophthalmic Implants for Treating Glaucoma

Samet ÖZDEMİR<sup>1\*</sup>, Egemen ÇAKIRLI<sup>2</sup>, Bilge SÜRÜCÜ<sup>2</sup>, Cemre İrem AYGÜLER<sup>2</sup>, Burcu ÜNER<sup>3</sup>, Ali Rıza Cenk ÇELEBİ<sup>4</sup>

<sup>1</sup>Istanbul Health and Technology University, Faculty of Pharmacy, Department of Pharmaceutical Technology, İstanbul, Türkiye

<sup>2</sup>Acıbadem University, Faculty of Pharmacy, Department of Pharmaceutical Technology, İstanbul, Türkiye

<sup>3</sup>Yeditepe University, Faculty of Pharmacy, Department of Pharmaceutical Technology, İstanbul, Türkiye

<sup>4</sup>Acıbadem University, Faculty of Medicine, Department of Ophthalmology, İstanbul, Türkiye

## ABSTRACT

**Objectives:** This study constructed dorzolamide (DRZ)-loaded ophthalmic implants for extended drug delivery and increased drug retention.

**Materials and Methods:** Carboxymethyl cellulose (CMC) and chitosan (CHI) were used to describe the ophthalmic implants. The implants were prepared by the solvent casting technique in presence of polyethylene glycol 6000 (PEG 6000) as plasticizer. Physicochemical characterization studies including mechanical characteristics [tensile strength (TS), elongation at break, and Young's modulus], bioadhesion studies, and *in vitro* and *ex vivo* drug release studies were conducted.

**Results:** TS of drug-loaded ophthalmic implants was 10.70 and 11.68 MPa, respectively. Elongation at break of CMC and CHI implants was 62.00% and 59.05%, respectively. The *in vitro* release profiles fit into Higuchi type kinetic model. *Ex vivo* release study results for both implants were correlated with *in vitro* release investigations.

**Conclusion:** CMC and CHI-based implants provide extended drug delivery. Implants prepared using CMC provided a significantly slower *in vitro* release rate, and drug retention on ocular surfaces increased. Thus, it has been concluded that DRZ-loaded CMC implants could provide effective treatment for glaucoma.

**Key words:** Dorzolamide, carboxymethyl cellulose, chitosan, ocular implant

## INTRODUCTION

Glaucoma is a progressive optic neuropathy resulting from high intraocular pressure (IOP). This condition is stated as the main reason for irreversible blindness after diabetic retinopathy.<sup>1</sup> Purpose of the therapy is to prevent optic nerve damage. Glaucoma is treated with the use of drugs (pharmaceutical therapy). Pharmacologically, beta receptor antagonists, prostaglandin analogs, alpha-2 agonists, and carbonic anhydrase inhibitors are chosen as treatment options.<sup>2</sup> Dorzolamide (DRZ) is one of the carbonic anhydrase inhibitors that decreases the

secretion of aqueous humor, thus the IOP is lowered.<sup>3</sup> DRZ eye drop is available on the market under trade name Trusopt® (Merck, N.J., USA). The dosage form contains 2% DRZ aqueous buffered solution at pH 5.6. DRZ 2% eye drops have exhibited the highest and optimal therapeutic effect in clinical trials.<sup>4</sup>

Effective ocular delivery of drug substances is a challenging process. Topical ophthalmic solutions are mostly preferred preparations by clinicians due to their ease of application. However, topical conventional delivery systems remain insufficient due to multifactorial restrictions of the ocular

\*Correspondence: eczsametozdemir@gmail.com, Phone: +90 444 3 788, ORCID-ID: orcid.org/0000-0001-6212-2706

Received: 31.03.2022, Accepted: 09.08.2022



©Copyright 2023 by Turkish Pharmacists' Association / Turkish Journal of Pharmaceutical Sciences published by Galenos Publishing House.  
Licensed by Creative Commons Attribution-NonCommercial-NoDerivatives 4.0 (CC BY-NC-ND)

anatomy. These can be mainly categorized as intraocular microenvironment, static, dynamic, and metabolic barriers.<sup>5</sup> Intraocular environment includes blood-aqueous and blood-retina barriers. The static barriers include biological structures such as the corneal epithelium, sclera, and conjunctiva. The metabolic barriers contain metabolic enzymes. Dynamic barriers are listed as; blinking, tear turnover, and nasolacrimal drainage, which remarkably decrease the drug bioavailability.<sup>6</sup>

Many sophisticated strategies have been introduced for bypassing the ophthalmic barriers, such as nanoparticles for enhancement of corneal permeation<sup>7-9</sup> and liposomal carriers for enhancement of ocular absorption and precorneal retention.<sup>10,11</sup> Micro or nanoemulsions are used for increasing the precorneal residence time and providing sustained release.<sup>12,13</sup> Hydrogels and ocular inserts are used as primary or secondary delivery systems. The incorporation of nanocarriers into the hydrogels or ocular inserts makes them a secondary delivery system. Hydrogels or ocular inserts can be used as primary drug delivery systems for treating ophthalmic problems.<sup>14,15</sup>

Chitosan (CHI) and carboxymethyl cellulose (CMC) are biodegradable and bioadhesive polymers that are used for the production of hydrogel or ocular implant or insert formulations.<sup>16,17</sup> These polymers are compatible materials with drug substances and biological surfaces. In this study, we aimed to construct an ophthalmic implant for the extended delivery of DRZ to achieve efficient glaucoma treatment. For this purpose, polymeric ophthalmic implants were developed and physicochemically characterized, and then, *in vitro* and *ex vivo* drug release profiles were investigated.

## MATERIALS AND METHODS

### Materials

CMC and CHI were obtained from Sigma Aldrich (Germany). Polyethylene glycol 6000 (PEG 6000), acetic acid, potassium dihydrogen phosphate ( $K_2PO_4$ ), and methanol (MeOH) were acquired from Merck-Millipore (USA). DRZ was kindly donated by Deva Pharmaceuticals (Türkiye). The other materials were of analytical quality.

### Methods

#### Preparation of ophthalmic implants

CMC and CHI were used as polymers, PEG 6000 was selected as plasticizer (to provide elasticity) and DRZ was used as active pharmaceutical ingredient, which is dissolved in aqueous polymer-plasticizer dispersion. CMC-based implants include: CHI (1 g) was dispersed in 100 mL aqueous acetic acid solution (1%, w/w). CMC-based implants include: CMC (1 g) was dispersed in 100 mL of water. Both of the implant formulations have PEG 6000 (0.1 g) in 100 mL total dispersion volume to improve the mechanic properties.

The dispersions were poured into empty contact lens containers (1-Day Acuvue® moist contact lens container). The lens containers had a diameter of 14.2 mm and a space to hold a gram of mass. Dispersion-loaded containers were left for drying under the fume hood for 24 h at room temperature. According

to the placebo weight of containers, the amount of DRZ was adjusted and the strength was obtained as 2 mg DRZ/implant.

#### Analytical quantification of DRZ

Quantification of DRZ was performed using high performance liquid chromatography (HPLC) (Agilent 1100 series, Germany). The reported analytical method has been slightly changed.<sup>18</sup> In brief, HPLC was equipped with multiple wavelength ultraviolet/visible detectors. Separation was conducted by using a C-18 column (5  $\mu$ m, 4.6  $\times$  150 mm) (AgilentTech, Germany) at 25  $\pm$  0.5  $^{\circ}$ C.  $K_2PO_4$  (pH:2.5): MeOH mixture (90:10, v/v) was used as mobile phase. Quantification was achieved at a flow rate of 0.8 mL/min. This analytical method was validated using universal parameters.

#### Characterization studies of ocular implants

##### Bioadhesion studies

A previously stated technique was slightly adapted for ocular tissues.<sup>19</sup> Bioadhesive characteristics of implants were detected by applying a texture analyzer (TA-XT Plus Texture Analyzer, Stable Micro System, UK). Swine eyes were obtained from the laboratory animal center and, then, the cornea was isolated from the ocular tissues. The implant was stabilized on a probe of the instrument using adhesive tape and the cornea was placed on the other probe of the instrument. DRZ-loaded implant was contacted to the tissue. Time of contact, rate and applied force were 60 s, 1 mm/s, and 0.2 N, respectively. The work of bioadhesion has been calculated using force-distance graph.

##### Mechanical characteristics

Mechanical characteristics of ocular implants were investigated using a texture analyzer (TA-XT Plus Texture Analyzer, Stable Micro Systems, UK). Calibration of force was achieved using 2 kg weight and calibration of height was achieved for Tensile Grips (Stable Micro Systems, UK). The samples were arranged by cutting 10 mm  $\times$  10 mm were stabilized in grip with primary distance of 50 mm and crosshead speed kept at 2 mm/sec tension mode. Tensile strength (TS) in MPa was measured by dividing the peak load improved during the analysis by the film cross-sectional area. TS, MPa, maximum elongation percentage at break (EAB, %), and Young's modulus (YM, MPa) were computed using equations 1, 2, and 3, respectively. Tests were performed in triplicate and the outcomes were described as mean values ( $\pm$  standard deviation).

$$TS = \frac{F_{max}}{A} \quad (\text{equation 1})$$

$$EAB = \frac{L_{max}}{LO} \times 100 \quad (\text{equation 2})$$

$$YM = S \times \frac{LO}{A} \quad (\text{equation 3})$$

$F_{max}$  indicates the maximum force, A is implant cross-sectional area,  $L_{max}$  and LO are the maximum deformation before rupture and primary length, respectively, and S is the slope of force deformation.<sup>20</sup>

#### Fourier transform infrared spectroscopy (FTIR) analysis

The spectra of ocular implants were obtained in the range of 650–4000  $\text{cm}^{-1}$  by using an FTIR spectrometer (NICOLET iS50, Thermo Scientific, USA). Ocular implants were nicely divided and the specimens were directly applied over the crystal of the spectrometer. Scans were performed for each specimen and the force over the specimen was arranged to obtain satisfactory transmittance results.

#### Thermal analysis

A previous method was applied to detect the thermal behavior of all materials.<sup>21</sup> Specimens were arranged as small parts and (approximately 5 mg) transferred into covered aluminum pans. The temperature was elevated up to 300 °C under a cover of nitrogen gas (50 mL/s) with a heating rate of 10 °C/min using a differential scanning calorimetry (DSC) instrument (Setaram, DSC131, France).

#### Morphological analysis

Morphological analysis of ocular implants was achieved by using a scanning electron microscope (SEM) (Quattro S, Thermo Scientific, USA). SEM was used with an accelerating voltage of 15.00 kV and surfaces of the isolated specimens were covered with gold and palladium using a sputter (Leica EM ACE200, Leica Microsystems, Germany) at 3 kV for 60 s. SEM micrographs were captured by applying a high vacuum.

#### Solubility studies

Before the *in vitro* and *ex vivo* studies, solubility of DRZ was investigated using a previously described method.<sup>19</sup> Briefly, an excessive amount of DRZ was added into flasks (10 mL volume of each) that contained distilled water (pH: 7), phosphate buffer (pH: 7.4), and normal saline (NS) solution (0.9% NaCl, pH: 5.5). The flasks were shaken for 48 h and saturated solutions were filtered through 0.22  $\mu\text{m}$  filters and quantified using HPLC.

#### *In vitro* drug release

*In vitro* DRZ-release profile was investigated using a previously reported paddle over disk method.<sup>21</sup> The specimens were placed in vessels that contained a 250 mL phosphate buffer solution (PBS) at pH 7.4. Temperature was kept constant at 37.5 °C. At pre-determined time intervals 2 mL samples were withdrawn from the release medium and completed with the same volume of fresh buffer solution. The samples were analyzed using the validated HPLC method. Release kinetics were also assessed by using zero-order, first-order, Hixson Crowell, Higuchi, and Korsmeyer-Peppas models.

#### *Ex vivo* studies

*Ex vivo* studies were conducted by using removed swine eyes. The eyes were placed into a small beaker (25 mL volume), and 20 mL buffer solution (pH 7.4) was added to cover the surface of the eye. Then, the ophthalmic implant was placed on the eye. At pre-determined time intervals, 1 mL of sample was withdrawn and replenished using fresh buffer.

An eye drop of DRZ was prepared using NS solution-DRZ at 2% (w/v) concentration. Similarly, the same *ex vivo* protocol was applied to the eye drops. Briefly, 2 drops (2 mg of DRZ) of preparation were applied to the swine eyes (placed in 20 mL buffer solution at pH 7.4). At pre-determined time intervals, 1 mL of sample was withdrawn and replenished using fresh buffer.

#### Statistical analysis

The samples were analyzed using the HPLC method. Then, the amount of drug penetrated was calculated retrospectively.

## RESULTS AND DISCUSSION

#### Preparation of ophthalmic implants

Ophthalmic implants in the shape of convex ocular hemispheres were prepared using a previously generated solvent casting method.<sup>21</sup> This technique involves preparing a polymer dispersion, which is poured onto a concave mold (empty contact lens containers). Then, the solvent was removed by evaporation, which caused the reorganization of polymer molecules and engagement with each other. Finally, formation of films was achieved by this phenomenon. After solvent casting, implants had a similar surface with the mold shape. They were dry, elastic, and transparent films. Elastic films were easily removed from the contact lens containers (molds), probably because of the presence of plasticizer.

#### Mechanical characteristics

Mechanical characteristics of the specimens, including TS, EAB, and YM, are presented in Table 1. EAB is defined as the ability of a film to extend before it breaks. For that reason, if EAB is high, the structure of the implant might be thought to be flexible and soft.<sup>22</sup> TS is described as the maximum load power used to break the film. Rigid and fragile materials exhibit high resistance.<sup>23</sup> EAB and TS of unloaded CMC films were 71.68% and 7.81 MPa, respectively, and the values of loaded CMC films were 62.00% and 10.70 MPa, respectively. Similar values are also available for CHI films; unloaded CHI films were 69.78% and 8.21 MPa, respectively, and the values of loaded CHI films were

**Table 1. Mechanical characteristics of inserts**

Samples	The work of bioadhesion ( $\text{mJ}/\text{cm}^2$ )	TS (MPa)	YM (MPa)	EAB (%)
CMC 1% unloaded	0.143 $\pm$ 0.046	7.81 $\pm$ 0.017	10.77 $\pm$ 0.317	71.68 $\pm$ 0.049
CMC 1% loaded	0.427 $\pm$ 0.163	10.70 $\pm$ 0.031	13.80 $\pm$ 0.226	62.00 $\pm$ 0.03
CHI 1% unloaded	0.255 $\pm$ 0.032	8.21 $\pm$ 0.02	11.32 $\pm$ 0.165	69.78 $\pm$ 0.211
CHI 1% loaded	0.434 $\pm$ 0.072	11.68 $\pm$ 0.012	14.39 $\pm$ 0.244	59.05 $\pm$ 0.101

CHI: Chitosan, CMC: Carboxymethyl cellulose, TS: Tensile strength, YM: Young's modulus, EAB: Elongation percentage at break

59.05% and 11.68 MPa, respectively. Decline of the EAB and increment of the TS could be explained as the drug molecules interposed the linkages of the polymers.

Similar formulations based on CMC were investigated and it was observed that mechanical properties changed according to the concentration of the active substance. In a study, 1% (w/w) of CMC film was developed with different concentrations of active substance and it was found that addition of active substance increases TS of lean film from 17.75 MPa to 58.85 MPa. Also, the amount of casting mass and thickness of the final formulation has a direct effect on the mechanical properties. The increment of mechanical strength is compatible with literature data.<sup>24</sup>

For mechanical assessment of CHI-based formulations, it was observed that polymer concentration and active substance amount had direct impacts on the mechanical properties. In a study, thin film formulations of CHI have been prepared. Then, it was found that mechanical strength has been elevated (7.1 N, 21.6 N, 36.5 N) by increased polymer concentrations (1%, 1.5%, and 2%) and elastic properties were found to be declined. In the same report, it was observed that incorporation of the active substance exhibited similar mechanical behavior.<sup>25</sup>

In the pre-formulation part, it is not possible to remove the lean implants (containing only polymers) from the molds because of their fragility. Thus, plasticizer (PEG 6000) was added onto the lean CMC and CHI dispersions to augment mechanical characteristics. YM is related to film rigidity and ability to undergo elastic deformation under applied stress.<sup>23</sup> Addition of DRZ increased the YM. The data gathered from mechanical experiments (EAB, TS, and YM) has been correlated with each other.

Bioadhesive assessment of the implant formulations is demonstrated in Table 1. Unloaded implants exhibited a lesser work of bioadhesion than loaded formulations. Thus, drug-loaded formulations could be promising delivery systems for eye. Chemical structure of the drug substance in salt form may, thus, affect the bioadhesive properties of implants. Existence of salts has been reported as one of the factors that affect the bioadhesive properties of polymeric drug delivery systems for topical or mucosal administration.<sup>26</sup>

*In vivo* bioadhesion mechanism of the polymeric films can be explained by the interaction with tear fluid or meibum, which is secreted from holocrine meibomian glands.<sup>27</sup> The early stages of mucosal adhesion include hydration of the polymer *via* normal physiological conditions of the eye surface. The hydrogen bonding capacity of polymers (CMC and CHI) also contributed to mucosal adhesion due to the presence of hydroxyl groups. This functional group has also contributed to the wettability and hydration. Physiologically, the contents of meibum (ester content) could have great potential to increase adhesion properties *in vivo*.

#### FTIR analysis

FTIR reflects the interactions between the contents of ocular implants and DRZ. These possible interactions will directly affect the characteristics of the ocular implant.<sup>3</sup> FTIR spectra of unloaded CMC and CHI implants treated with DRZ are shown

in Figure 1. Four inserts exhibited similar main peaks, but the amplitude varied dramatically with some of them moving. Figure 1 depicts FTIR spectra of the inserts. In DRZ spectrum, the characteristic SO<sub>2</sub> bonds of sulphonamide shifted from 1342 cm<sup>-1</sup> to 1782 cm<sup>-1</sup> and 1766 cm<sup>-1</sup> for 1% CMC-DRZ and 1% CHI, respectively. Other characteristic bands of -NH<sub>2</sub><sup>+</sup> stretching at 1281 cm<sup>-1</sup>, shifted to 1396 cm<sup>-1</sup> for 1% CHI-DRZ and became widespread for 1% CMC-DRZ.<sup>28,29</sup> 1% CMC-DRZ and 1% CHI-DRZ spectra indicated that the peak intensities of CMC were better than those of CHI formulations. In % CHI spectrum, the characteristic bands of -CH<sub>2</sub> stretching at 1083 cm<sup>-1</sup> became widespread for 1% CHI-DRZ and % CHI spectra, and the characteristic bands of -C=O stretching at 1603 cm<sup>-1</sup>, intensity decreased with the addition of DRZ for % CHI-DRZ.<sup>30,31</sup> The peak intensity of the films with DRZ was better than those of the films without DRZ. In addition, the double spectra at 2900-2800 cm<sup>-1</sup> observed in both CMC and CHI formulations are due to the vibrations of -COO group in CMC and CHI.<sup>32</sup> Therefore, we confirmed that addition of DRZ to and use of CMC film can facilitate uniform mixing in the film.

#### DSC analysis

Determination of solid-state interactions has been performed using DSC. The thermograms are shown in Figure 2 and melting points, enthalpies, and crystallinity indices are presented in Table 2. The enthalpy values of DRZ, CMC 1%, CMC-DRZ 1%, CHI 1%, and CHI-DRZ 1% were 9.455, 29.016, 28.702, 23.892, and 21.233 J/g, respectively, while the melting temperatures of DRZ, CMC 1%, CMC-DRZ 1%, CHI 1%, and CHI-DRZ 1% were 260.41, 219.82, 206.56, 249.14, and 239.53 °C, respectively.

Table 2 displays that results proved the CMC of amorphous structure of polymers and obstructed crystallization.<sup>33,34</sup> Melting points of ocular films have exposed a decline to lower temperatures with larger peaks compared to the bulk polymer by giving variable enthalpy values indicating several thermal transitions as well.<sup>35</sup> A decline in the melting points of the CHI 1% and CHI-DRZ 1% formulations was detected at 10 °C, when CMC was added instead of CHI, causing a greater decrease in CMC 1% and CMC-DRZ 1%. Reduction in CI of CMC 1% and CMC-DRZ

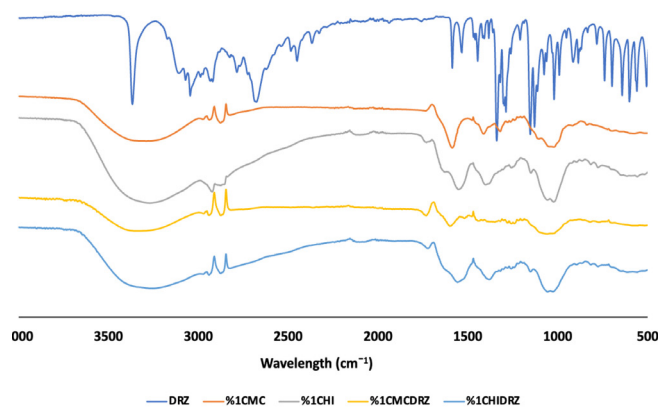


**Figure 1.** FTIR spectra of active substance and formulations  
FTIR: Fourier transform infrared spectroscopy

1% compared to CHI 1% and CHI-DRZ 1% could be attributed to the crystal order in CMC 1% and CMC-DRZ 1% greatly disturbed due to CMC. In a study, salicylic acid was loaded into the CHI-based films and it was reported that the crystallization index of the salicylic acid-loaded formulations increased by about 10% compared to the unloaded films.<sup>36</sup>

#### SEM analysis of ocular implants

Images of ocular inserts are presented in Figure 3. Obtained data verify that surface of the designed inserts is smooth and plain. Therefore, it could be considered that the implants would not block vision.

#### In vitro drug release

*In vitro* drug release profile of a drug delivery system is an important parameter for noticing *in vivo* action of a drug substance. Generally, release experiments are accomplished under sink conditions. European Pharmacopeia describes the sink conditions as a volume of release medium that is at least three to ten times of the active ingredient saturation volume.<sup>37</sup> The solubility of DRZ was found to be 6.65 mg/mL, 6.72 mg/

mL, and 38.76 mg/mL in distilled water (pH: 7), phosphate buffer (pH: 7.4), and NS solution (pH: 5.5), respectively. The obtained solubility data agreed with the literature.<sup>38,39</sup> After that, the volume of release medium and content was determined and other parameters were selected by considering normal physiological conditions.

According to the mathematical analysis of *in vitro* release studies (Table 3, Figure 4), the profiles fitted Higuchi-type kinetic model. As indicated in the literature, Higuchi-type release kinetics could express the drug release from polymeric matrices.<sup>40</sup> Moreover, there were some assumptions reported for Higuchi type kinetics, in this case the probable assumptions could be: (i) drug diffusion is one-dimensional, making effects of margins negligible, (ii) the diffusivity of the drug is fixed, (iii) perfect sink conditions are reached.<sup>40,41</sup>

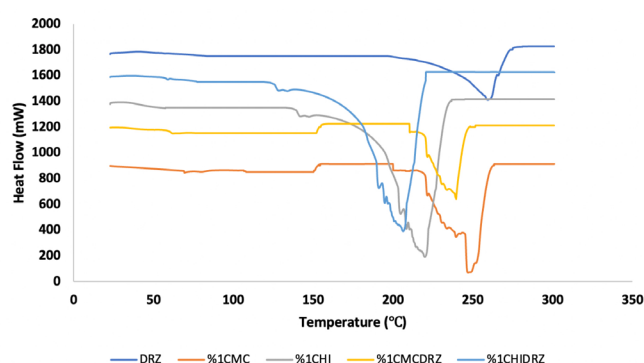


**Figure 2.** DSC curves of DRZ, CMC 1%, CMC-DRZ 1%, CHI 1%, and CHI-DRZ 1%

DSC: Differential scanning calorimetry, DRZ: Dorzolamide, CHI: Chitosan, CMC: Carboxymethyl cellulose

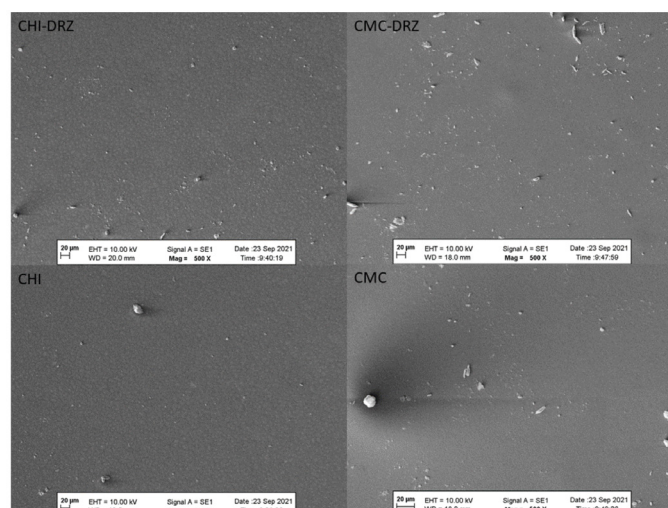


**Figure 3.** SEM images of the DRZ loaded (CHI-DRZ; CMC-DRZ) and unloaded (CHI; CMC) implants

SEM: Scanning electron microscope, DRZ: Dorzolamide, CHI: Chitosan, CMC: Carboxymethyl cellulose

**Table 2.** Thermal parameters of active substance and films

Formulations	Melting point (°C)	Enthalpy $\Delta H$ (J/g)	Crystallinity index (%)
DRZ	260.41	9.455	100
CMC 1%	219.82	29.016	32.57
CMC-DRZ 1%	206.56	28.702	32.94
CHI 1%	249.14	23.892	39.58
CHI-DRZ 1%	239.53	21.233	44.529

DRZ: Dorzolamide, CHI: Chitosan, CMC: Carboxymethyl cellulose

**Table 3.** Kinetic models of formulations

	Zero order (R <sup>2</sup> )	First order (R <sup>2</sup> )	Higuchi (R <sup>2</sup> )	Korsmeyer-Peppas (R <sup>2</sup> )	(n)	Hixson-Crowell (R <sup>2</sup> )
1.0% CMC-DRZ	0.8156	0.7312	0.9733	0.9313	0.301	0.9461
1.0% CHI-DRZ	0.9352	0.6447	0.9918	0.7818	0.243	0.9172

R<sup>2</sup>: Correlation coefficient, n: Release exponent

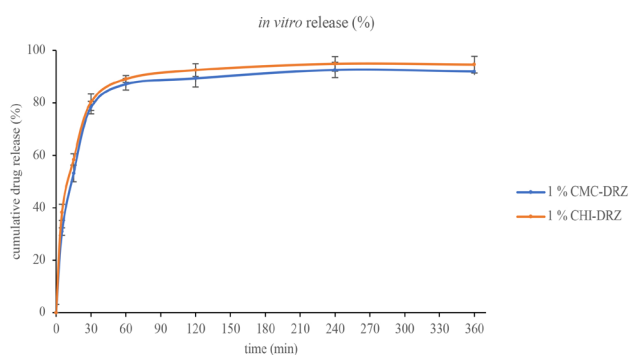


Figure 4. *In vitro* release profile of ocular implants

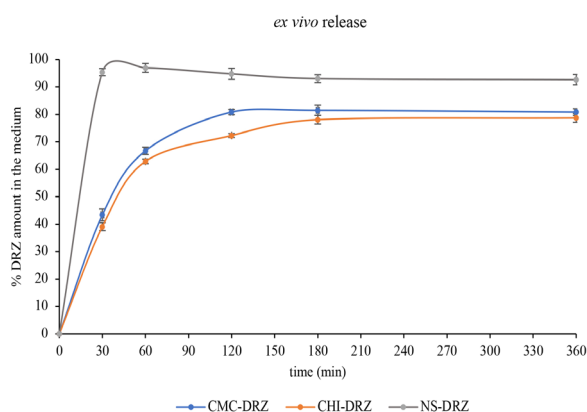


Figure 5. *Ex vivo* release profile of ocular implants

Polymer type and molecular weight directly change release profile of formulations. A similar study investigated the release patterns of sodium alginate, hydroxypropyl methylcellulose (HPMC), and CHI-based ocular inserts loaded with brimonidine.<sup>42</sup> CHI and HPMC based inserts exhibited more than 80% of drug release *in vitro* in the first 30 mins. The sodium alginate based formulations exhibited approximately 80% of drug release *in vitro* in the first 120 mins. The goal of this study was to observe the prolongation of drug contact with the ocular tissue by using biodegradable polymeric systems for daily application. Thus, the amount of DRZ was calculated (2 mg DRZ/implant) according to the dose of the market product's daily application.

#### *Ex vivo* release study

*Ex vivo* drug release profile of dosage form reflects the passage or retention of drug substances throughout the tissue. The applied method detects the residual drug amount on the release medium. Thus, the plateau levels at the 3<sup>rd</sup> and 6<sup>th</sup> hours indicate the drug saturation levels (Figure 5). The eye drop (NS-DRZ, 2% DRZ) exhibited instant drug payload in the first 30 min (95.4% ± 1.3), then release percentages of NS-DRZ were found as 93.04% and 92.66% at 3<sup>rd</sup> and 6<sup>th</sup> hours, respectively. It was considered that 7.34% of the drug was retained or passed throughout *ex vivo* tissue. The release percentages of CMC-DRZ were 81.5% and 80.9% at 3<sup>rd</sup> and 6<sup>th</sup> hours, respectively. The release percentages of CHI-DRZ were 78.1% and 78.7% at 3<sup>rd</sup> and 6<sup>th</sup> hours, respectively. Thus, *ex vivo* release outcomes are

correlated with *in vitro* release studies. The implants designed with CHI have shown slightly faster *in vitro* release rate, so they could cause faster retention outside *ex vivo* tissues. Between 21.3% and 18.5% of the drug was estimated as retained or passed throughout *ex vivo* tissue.

As previously stated, physiological factors hinder ocular drug absorption and bioavailability.<sup>5,6</sup> It was reported that less than 5% of the applied dose is absorbed into ocular tissues.<sup>39</sup> Therefore, nanoparticulated systems, *in situ* gelling systems, and biodegradable polymeric systems were developed to increase drug permeation, extend the presence of drug substances in ocular tissues, and prolong drug release. NS-DRZ (representing the traditional application) implant exhibits 2.5 and 3.0 fold lower *ex vivo* drug absorption than CMC-DRZ and CHI-DRZ implants.

## CONCLUSION

Ophthalmic implants showed remarkable results in both *in vitro* and *ex vivo* investigations for better ophthalmic drug delivery in this study. DRZ-loaded CMC and CHI ocular implants were prepared in the shape of transparent hemispheres; so as not to interfere with the vision. *Ex vivo* release data are correlated with *in vitro* release outcomes. The implant-designed CHI exhibited a slightly faster *in vitro* release rate, so it could cause faster retention in the ocular tissues. DRZ release from implants was biphasic with an initial release lasting about 2 h and then a continuous release lasting up to 6 h. It can be inferred that DRZ-loaded ocular implants can be an effective ocular delivery strategy.

#### Ethics

**Ethics Committee Approval:** Not applicable.

**Informed Consent:** Not applicable.

**Peer-review:** Externally peer-reviewed.

#### Authorship Contributions

Surgical and Medical Practices: A.R.C.Ç., Concept: A.R.C.Ç., Design: S.Ö., B.Ü., A.R.C.Ç., Data Collection or Processing: E.Ç., B.S., C.İ.A., Analysis or Interpretation: E.Ç., B.S., C.İ.A., Literature Search: S.Ö., B.Ü., Writing: S.Ö., A.R.C.Ç.

**Conflict of Interest:** No conflict of interest was declared by the authors.

**Financial Disclosure:** The authors declared that this study received no financial support.

## REFERENCES

- Lang GK. Ophthalmology: a short textbook. New York; Thieme Medical Publishers; 2000.
- Abel SR, Sorensen SJ. Eye disorders. In: Koda-Kimble MA, eds., Koda-Kimble and Young's applied therapeutics: the clinical use of drugs. Wolters Kluwer Health/Lippincott Williams & Wilkins; 2012:1301-1322.
- Scozzafava A, Supuran CT. Glaucoma and the applications of carbonic anhydrase inhibitors. Subcell Biochem. 2014;75:349-359.
- Donohue EK, Wilensky JT. Trusopt, a topical carbonic anhydrase inhibitor. J Glaucoma. 1996;5:68-74.

5. Suri R, Beg S, Kohli K. Target strategies for drug delivery bypassing ocular barriers. *J Drug Deliv Sci Technol.* 2020;55:101389.
6. Bachu RD, Chowdhury P, Al-Saedi ZHF, Karla PK, Boddu SHS. Ocular drug delivery barriers-role of nanocarriers in the treatment of anterior segment ocular diseases. *Pharmaceutics.* 2018;10:28.
7. Güven UM, Yenilmez E. Olopatadine hydrochloride loaded Kollidon® SR nanoparticles for ocular delivery: nanosuspension formulation and *in vitro-in vivo* evaluation. *J Drug Deliv Sci Technol* 2019;51:506-512.
8. Ustündağ-Okur N, Gökçe EH, Bozbiyık Dİ, Eğrilmez S, Ozer O, Ertan G. Preparation and *in vitro-in vivo* evaluation of ofloxacin loaded ophthalmic nano structured lipid carriers modified with chitosan oligosaccharide lactate for the treatment of bacterial keratitis. *Eur J Pharm Sci.* 2014;63:204-215.
9. Vega E, Egea MA, Valls O, Espina M, García ML. Flurbiprofen loaded biodegradable nanoparticles for ophthalmic administration. *J Pharm Sci.* 2006;95:2393-2405.
10. Zhang J, Wang S. Topical use of coenzyme Q10-loaded liposomes coated with trimethyl chitosan: tolerance, precorneal retention and anti-cataract effect. *Int J Pharm.* 2009;372:66-75.
11. He W, Guo X, Feng M, Mao N. *In vitro* and *in vivo* studies on ocular vitamin A palmitate cationic liposomal *in situ* gels. *Int J Pharm.* 2013;458:305-314.
12. Kesavan K, Kant S, Singh PN, Pandit JK. Mucoadhesive chitosan-coated cationic microemulsion of dexamethasone for ocular delivery: *in vitro* and *in vivo* evaluation. *Curr Eye Res.* 2013;38:342-352.
13. Singh M, Bharadwaj S, Lee KE, Kang SG. Therapeutic nanoemulsions in ophthalmic drug administration: concept in formulations and characterization techniques for ocular drug delivery. *J Control Release.* 2020;328:895-916.
14. Pakzad Y, Fathi M, Omid Y, Mozafari M, Zamanian A. Synthesis and characterization of timolol maleate-loaded quaternized chitosan-based thermosensitive hydrogel: a transparent topical ocular delivery system for the treatment of glaucoma. *Int J Biol Macromol.* 2020;159:117-128.
15. Li B, Wang J, Gui Q, Yang H. Drug-loaded chitosan film prepared *via* facile solution casting and air-drying of plain water-based chitosan solution for ocular drug delivery. *Bioact Mater.* 2020;5:577-583.
16. Franca JR, Foureaux G, Fuscaldi LL, Ribeiro TG, Castilho RO, Yoshida MI, Cardoso VN, Fernandes SOA, Cronemberger S, Nogueira JC, Ferreira AJ, Faraco AAG. Chitosan/hydroxyethyl cellulose inserts for sustained-release of dorzolamide for glaucoma treatment: *in vitro* and *in vivo* evaluation. *Int J Pharm.* 2019;570:118662.
17. Andrews GP, Gorman SP, Jones DS. Rheological characterisation of primary and binary interactive bioadhesive gels composed of cellulose derivatives designed as ophthalmic viscosurgical devices. *Biomaterials.* 2005;26:571-580.
18. Park CG, Kim YK, Kim SN, Lee SH, Huh BK, Park MA, Won H, Park KH, Choy YB. Enhanced ocular efficacy of topically-delivered dorzolamide with nanostructured mucoadhesive microparticles. *Int J Pharm.* 2017;522:66-73.
19. Karakucuk A, Tort S. Preparation, characterization and antimicrobial activity evaluation of electrospun PCL nanofiber composites of resveratrol nanocrystals. *Pharm Dev Technol.* 2020;25:1216-1225.
20. Nawab A, Alam F, Haq MA, Lutfi Z, Hasnain A. Mango kernel starch-gum composite films: physical, mechanical and barrier properties. *Int J Biol Macromol.* 2017;98:869-876.
21. Özdemir S, Karaküçük A, Çakırlı E, Sürücü B, Üner B, Barak TH, Bardakçı H. Development and characterization of *Viburnum opulus* L. extract-loaded orodispersible films: potential route of administration for phytochemicals. *J Pharm Innov.* 2022;1-2.
22. Banker GS. Film coating theory and practice. *J Pharm Sci.* 1966;55:81-89.
23. Dixit RP, Puthli SP. Oral strip technology: overview and future potential. *J Control Release.* 2009;139:94-107.
24. Dashipour A, Razavilar V, Hosseini H, Shojaee-Aliabadi S, German JB, Ghanati K, Khakpour M, Khaksar R. Antioxidant and antimicrobial carboxymethyl cellulose films containing *Zataria multiflora* essential oil. *Int J Biol Macromol.* 2015;72:606-613.
25. Sezer AD, Hatipoğlu F, Cevher E, Oğurtan Z, Baş AL, Akbuğa J. Chitosan film containing fucoidan as a wound dressing for dermal burn healing: preparation and *in vitro/in vivo* evaluation. *AAPS PharmSciTech.* 2007;8:39.
26. Khan S, Trivedi V, Boateng J. Functional physico-chemical, *ex vivo* permeation and cell viability characterization of omeprazole loaded buccal films for paediatric drug delivery. *Int J Pharm.* 2016;500:217-226.
27. Rantamäki AH, Seppänen-Laakso T, Oresic M, Jauhiainen M, Holopainen JM. Human tear fluid lipidome: from composition to function. *PLoS One.* 2011;6:e19553.
28. Natu MV, Gaspar MN, Fontes Ribeiro CA, Cabrita AM, de Sousa HC, Gil MH. *In vitro* and *in vivo* evaluation of an intraocular implant for glaucoma treatment. *Int J Pharm.* 2011;415:73-82.
29. Papadimitriou S, Bikiaris D, Avgoustakis K, Karavas E, Georgarakis M. Chitosan nanoparticles loaded with dorzolamide and pramipexole. *Carbohydr Polym.* 2008;73:44-54.
30. Cardenas G, Miranda S. FTIR and TGA studies of chitosan composite films. *J Chil Chem Soc.* 2004;49:291-295.
31. Cuba-Chiem LT, Huynh L, Ralston J, Beattie DA. *In situ* particle film ATR FTIR spectroscopy of carboxymethyl cellulose adsorption on talc: binding mechanism, pH effects, and adsorption kinetics. *Langmuir.* 2008;24:8036-8044.
32. Dumont VC, Mansur AAP, Carvalho SM, Medeiros Borsagli FGL, Pereira MM, Mansur HS. Chitosan and carboxymethyl-chitosan capping ligands: effects on the nucleation and growth of hydroxyapatite nanoparticles for producing biocomposite membranes. *Mater Sci Eng C Mater Biol Appl.* 2016;59:265-277.
33. Rangelova N, Aleksandrov L, Angelova T, Georgieva N, Müller R. Preparation and characterization of SiO<sub>2</sub>/CMC/Ag hybrids with antibacterial properties. *Carbohydr Polym.* 2014;101:1166-1175.
34. Ikhuria E, Omorogbe S, Agbonlahor O. Spectral analysis of the chemical structure of carboxymethylated cellulose produced by green synthesis from coir fibre. *Ciênc e Tecnol dos Mater.* 2017;29:55-62.
35. Bonilla Lagos MJ, Bittante AMQB, Sobral PJdA. Thermal analysis of gelatin-chitosan edible film mixed with plant ethanolic extracts. *J Therm Anal Calorim.* 2017;130:1221-1227.
36. Puttipipatkachorn S, Nunthanid J, Yamamoto K, Peck GE. Drug physical state and drug-polymer interaction on drug release from chitosan matrix films. *J Control Release.* 2001;75:143-153.
37. Liu P, De Wulf O, Laru J, Heikkilä T, van Veen B, Kiesvaara J, Hirvonen J, Peltonen L, Laaksonen T. Dissolution studies of poorly soluble drug nanosuspensions in non-sink conditions. *AAPS PharmSciTech.* 2013;14:748-756.

38. Loftsson T, Jansook P, Stefánsson E. Topical drug delivery to the eye: dorzolamide. *Acta Ophthalmol.* 2012;90:603-608.
39. Sigurdsson HH, Stefánsson E, Gudmundsdóttir E, Eysteinnsson T, Thorsteinsdóttir M, Loftsson T. Cyclodextrin formulation of dorzolamide and its distribution in the eye after topical administration. *J Control Release.* 2005;102:255-262.
40. Bruschi ML. Mathematical models of drug release, in strategies to modify the drug release from pharmaceutical systems Ed. 2015, Woodhead Publishing, 2015;63-86.
41. Peppas NA, Narasimhan B. Mathematical models in drug delivery: how modeling has shaped the way we design new drug delivery systems. *J Control Release.* 2014;190:75-81.
42. Aburahma MH, Mahmoud AA. Biodegradable ocular inserts for sustained delivery of brimonidine tartarate: preparation and *in vitro/in vivo* evaluation. *AAPS PharmSciTech.* 2011;12:1335-1347.